05

Superconducting subterahertz range oscillators: history and new developments

© F.V. Khan,[1,2] L.V. Filippenko,[1] A.B. Ermakov,[1] N.V. Kinev,[1] V.P. Koshelets[1]

Kotelnikov Institute of Radio Engineering and Electronics, Russian Academy of Sciences,
125009 Moscow, Russia
[2]Moscow Institute of Physics and Technology (National Research University), 141701 Dolgoprudny, Moscow region, Russia
e-mail: valery@hitech.cplire.ru

Received April 21, 2025
Revised April 21, 2025
Accepted April 21, 2025

The paper presents the results of development a new type of oscillators based on arrays of Josephson junctions included in a superconducting coplanar line. Subterahertz range (200−700 GHz) oscillators based on arrays of tunnel Josephson junctions Nb−AlOx−Nb and Nb−AlN−NbN shunted by a thin-film resistor are investigated. Several series of oscillator's samples are manufactured, including arrays of 100, 200, 350 and 600 Josephson junctions with an area of $2.8\,\mu m^2$ and $4.2\,\mu m^2$. Studies of superconducting oscillators using integrated radiation detectors have shown the possibility of frequency tuning in the entire operating range up to 700 GHz with an output power of up to $0.4\,\mu W$ for an array of 600 junctions with a tunnel current density of $7\,kA/cm^2$, which is sufficient for applications in superconducting integrated receivers. The use of a superconducting harmonic mixer made it possible to measure the radiation spectrum of a superconducting oscillator at frequencies up to 700 GHz in the frequency stabilization mode and to implement the phase-locked loop mode. Further prospects in the field of developing superconducting oscillators in the terahertz range are discussed.

Keywords: Superconducting devices, superconductor-insulator-superconductor tunnel junction, subTHz range oscillators, shunted Josephson junction arrays.

DOI: 10.61011/TP.2025.09.61837.72-25

Introduction

Superconductor electronics devices based on tunnel superconductor–insulator–superconductor Josephson junctions (SIS) play an important role in many applied and fundamental studies. Operating frequencies in the terahertz (THz) range and cryogenic temperature make it possible to achieve a set of unique characteristics that are impossible for devices based on other operating principles. Strong nonlinearity near the gap frequency of the SIS junctions [1] makes them irreplaceable elements for superconducting mixers in heterodyne receivers with a noise temperature close to a value of the quantum limit $T_n = hf/2k_B$ [1,2]. We should also note a low level of intrinsic noise of the receiver elements, which is achieved due to operation at the cryogenic temperatures, as well as frequency convertibility with amplification in the SIS mixers.

Receivers based on superconducting elements are used in ground [3,4] and space [5,6] radio astronomy, when monitoring an atmosphere composition [7,8] and in other fundamental studies and applied fields. At the same time, a local oscillator for heterodyne receiver can be integrated together with the mixer in one chip [7,8], thereby making it possible to significantly increase efficiency of the devices.

The heterodyne oscillator for the superconducting terahertz-range receivers shall provide continuous tuning of the frequency within the entire range of operation of the SIS mixer and power sufficient for its pump as well as high spectral quality and low phase noises. Weight and size characteristics and energy consumption of this heterodyne oscillator are very important for space applications. Now, for the most SIS receivers the heterodyne is provided by a system of multipliers and power amplifiers [9,10], which can obtain the power of up to 2 mW at the frequency of 1 THz with efficiency of 5 % [9]. At the same time, the THz-range heterodynes that are suitable for operation when they are included in space telescopes, can be manufactured only in several scientific centers of USA and Europe. Therefore, it is fundamentally important for Russia-created cryogenic receivers [11] to design alternatives of the heterodyne, wherein one of the most promising options herein is a superconducting THz-range oscillator.

Works on creation and research of the subterahertz range oscillators based on superconducting junctions have been still underway since discovery of the Josephson effect. However, until recently, only the systems based on long Josephson junctions (LJJ) have in one device combined both terahertz oscillation with frequency tuning within the wide range as well as a narrow radiation linewidth required for practical use of such oscillators. The LJJ is one of the most studied types of the Josephson oscillators [11,12]; it is a long tunnel SIS junction (of a length much larger than the Josephson depth of penetration of the magnetic field into a contact λ_J), wherein the applied magnetic field and a bias current create a unidirectional flux of Josephson vortices, while each of them contains one quantum of the magnetic

flux. In modern superconducting integrated receivers, the LJJ is usually used as the generator.

The LJJ is a complex dynamic system, which can be accurately described only within the framework of a microscopic tunnel junction model [13]. The vortex dynamics depends both on a value of the magnetic field and the bias current that are applied to the junction as well as on radiation that propagates within the junction, which, in turn, depends on a degree of matching of the LJJ with a load [14]. Thus, to estimate the power and impedance of the LJJ, it is necessary to solve the self-consistent problem [13], where a supercomputer cluster was used for this purpose. Simpler models do not take into account many specific features, which turn out to be important in practice. Besides, a form of the current-voltage curve of the LJJ varies during thermal cyclings, therefore, even when using an automated system, pre-adjustment of the heterodyne requires some time (about 1 min) [7,12].

At the voltages below $V_g/3$ (V_g — a gap voltage of the tunnel junction), the LJJ operates in a Fiske steps resonance mode [15]. On the steps, differential resistance and, consequently, an autonomous width of the phase-locked loop mode line are quite small, thereby making it possible to quite simply select an operating point on the step. However, it is impossible to select the operating point when voltages are between the steps. Besides, when an electromagnetic wave propagates inside the LJJ at the frequencies above the Nb gap, a decay coefficient sharply increases, thereby limiting applicability, at the frequencies above 700 GHz, of the LJJ made according to the technology Nb–Al/AlO_x–Nb and even Nb–Al/AlN–NbN, in which only one electrode is made of niobium. It should be noted that using niobium nitride (NbN) with a critical temperature of about 15 K as a material of both the electrodes of the distributed tunnel junction will not solve all the problems. It is related to high surface resistance of the NbN films at the high frequency [16]. For this reason, the most receivers designed to operate at the frequencies above 700 GHz use other niobium compounds with smaller surface losses, for example, NbTiN. However, presently, there is no well-developed technology for producing high-quality tunnel junctions with the NbTiN electrodes.

An alternative is to use an array of N small (the size is much smaller than λ_J) Josephson junctions [17–26], thereby making it possible to get a gain in power in N times as compared to the single junction. Besides, provided that impedance of the external load is matched with the array impedance, there is also a decrease of the linewidth in N times [17,19], which is necessary for implementing a phase-locked loop (PLL) system in spectroscopy tasks. It should be noted that if the array is not matched with the load, then both power increase and decrease of the linewidth varies according to the law N^2 [19]. But in this case synchronization will be possible only at limited amount of the frequencies that correspond to geometrical resonances in the line. If the junction is in a wave node, then its oscillation frequency will be somewhat different from the others [20].

Results of investigation of one-dimensional and two-dimensional arrays of the Josephson junctions are given in the literature. Various arrangements of the junctions in the array were used: in groups at the distances that are equal to a half of the radiation wavelength [18] and regular arrangement of the junctions at the distance that is much less than the wavelength [23]. In the first case the radiation spectrum is limited by the geometrical resonances in the line; but at the same time it is possible to obtain oscillation of radiation of the power of up to 160 μW at the frequency of 240 GHz, which was demonstrated in the study [21] by means of a single-Josephson-junction detector with the oscillator in the same chip. This power is already enough for radiation into open space. It is simpler to achieve synchronization in this case, as all the junctions turn out to be in antinodes of the electromagnetic wave (they are arranged by groups in the array in $\lambda/2$). In the second case, the limitation related to the geometrical resonances is caused only by sizes of the entire array (the resonances become more frequent and have less quality factor), thereby making it possible to tune the frequency. The paper [25] provides results of investigation of the array that consists of 9996 junctions Nb/NbSi/Nb; while the operating frequencies are within the range from 139 to 343 GHz with a capability of continuous tuning of the frequency. The junctions can be synchronized by excitation of modes in a substrate. The radiation linewidth in the best point is below 1 MHz. The main parameters and characteristics of the oscillators on the arrays studied in the papers [21–25] are given in Table. In all the papers, except for [24,25], the output power was measured by means of a detector that was arranged in the same chip as the studied array.

The present study is dedicated to investigation of the subTHz-range superconducting oscillators that are based on the one-dimensional arrays of the tunnel SIS junctions Nb–AlO_x–Nb and Nb–AlN–NbN, which are shunted by thin-film resistors. A new array design is proposed, manufactured and studied, wherein the junctions are included in series and embedded into a central electrode of the coplanar line. As compared to the long Josephson junctions, an important advantage of these arrays for operation at the subTHz frequencies is significant reduction of the influence of losses in the superconducting electrodes due to a various configuration of high-frequency currents, which in the LJJ flow directly in an area of the tunnel junction. Using the coplanar line enables forming the line electrodes from materials with higher values of the critical temperature and the gap voltage (therefore, with small surface losses at the frequencies of about 1 THz), whereas the electrodes of the tunnel junctions themselves can be manufactured based on well-adjusted approaches and procedures. At the same time, it is possible to use the tunnel junctions with a very high current density despite significant deterioration of a quality parameter, since the tunnel junctions are shunted with an additional resistor. A technique of manufacturing the

Parameters of the oscillators based on the arrays from the papers [21–25]

Paper	Operating range, GHz	N	Maximum power, μW	Width of the oscillation line, MHz	Arrangement of the junctions
[21]	240	1968	160	No data available	1D, $l = \lambda/2$, groups
[22]	566, 625	11	10	8	1D, $l = \lambda/2$
[23]	200–500	20	1.5	10.3	1D, $l = \lambda/2$, groups
[24]	53–230	10×10	0.2	0.01	2D, $l \ll \lambda$
[25]	139–343	9996	3.0	1.5	1D, $l \ll \lambda$

Note.*groups means that the junctions within the group are at the distances $\ll \lambda$ from each other, while the distance between the groups $\lambda/2$.

experimental structures is described in Section 1. Section 2 is dedicated to description of integrated microcircuits for studying the superconducting oscillators. Section 3 provides a procedure of the measurements and the obtained results of investigation of the various array types. The optimized array design is described and the first results of measurement of these structures are given.

1. Description of the technological processes

The studied structures were manufactured using a technique that is multiply tested in V.A. Kotelnikov Institute of Radio Engineering and Electronics of Russian Academy of Sciences and includes processes of optical and electron-beam lithography, magnetron sputtering, reactive ion etching and lift-off lithography [27,28]. This technique was tested when manufacturing low-noise THz-range receivers for radio astronomy and integrated receivers designed for monitoring the atmosphere and laboratory applications [11,29]. The structures were manufactured by using equipment from Unique Scientific Unit „Cryointegral“–„Technology and Measurement Facility for Fabrication of Superconducting Nanosystems using New Materials“ [30]; this facility is unique and, in essence, the only one in the Russian Federation, in which it is possible to manufacture high-quality niobium-based tunnel junctions. In particular, the technique of manufacturing the three-layer structures $Nb-AlO_x-Nb$ makes it possible to produce the junctions with the gap voltage V_g of up to 2.85 mV and a ratio of the sub-gap resistance to the normal one, which exceeds 20, with good reproducibility of the parameters [27–29].

Let us shortly describe a technique of manufacturing the integrated superconducting structures based on the tunnel junctions $Nb-Al/AlO_x-Nb$; let us note that for the junctions based on aluminum nitride ($Nb-Al/AlN-NbN$) a process of oxidation of a thin aluminum film was replaced by a nitridation process, while instead of niobium nitride was used in the three-layer structure. The Al_2O_3 layer of the thickness of 100 nm is sputtered on the high-resistance-silicon substrate by high-frequency magnetron sputtering. Its main function is to protect the substrate surface when forming a lower electrode. Then the three-layer structure $Nb-Al/AlO_x-Nb$ was formed: a thin aluminum layer (7 nm) is sputtered to the lower niobium electrode of the thickness of 200 nm, which, when being oxidized in the oxygen atmosphere, makes it possible to produce a tunnel barrier of the thickness of 1 nm. The manufacturing of the three-layer structure is completed by sputtering with 70 nm of Nb. A topology of the three-layer structure is formed by lift-off lithography. Then, during plasma-enhanced chemical etching, the SIS junctions are formed in the mixture of CF_4 and O_2 At the same time, the aluminum layer prevents etching of the lower electrode. After oxidation, in order to prevent short-circuiting, the manufactured layers are anodized to form a thin oxide layer (about 10 nm) on the surfaces. After that, a silicon dioxide layer of the thickness of 250 nm is sputtered, which serves as an insulator in microstrip lines. Then, lift-off lithography is used to form thin-film molybdenum resistors of the thickness of 100 nm, the resistance is $\sim 1\Omega/\square$. Let us note that the shunt is directly connected to the lower electrode, rather than via the large-area SIS junction, and an additional etching operation is carried out for this purpose. Connection of the shunt via the SIS junction results in origination of additional resonances in the current-voltage curve of the oscillator, which are caused by excitation of oscillations at a plasma frequency of the junction. The process of manufacturing of the superconducting structure is completed by a stage of formation of the upper niobium-based electrode of the thickness of 350 nm, which is carried out by lift-off lithography. In order to connect to the experimental sample, a lift-off photolithography method is used to manufacture golden contact pads to the base (lower) and upper electrodes. An image of the technological layers near the SIS junction in the array together with the shunt is shown in Fig. 1.

2. Experimental samples

Fig. 2, *a* shows an image of one of the studied samples in the optical microscope and presents an array of the 100 shunted Josephson junctions. Fig. 2, *b* shows a magnified image of the SIS junctions in the array together with the shunts. The array is formed by junctions connected in series, wherein each of them is shunted by the thin-film

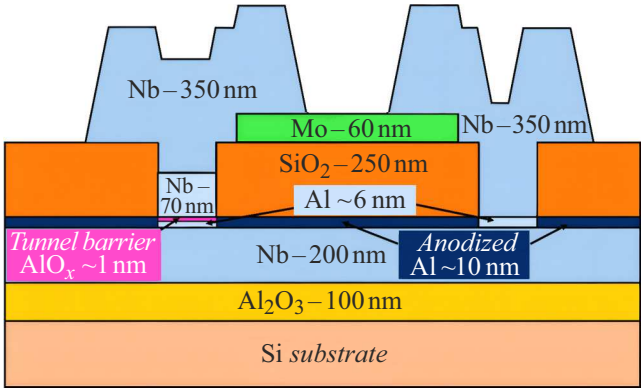

Figure 1. Image of the technological layers near one SIS junction in the array together with the shunt made of the normal metal (a position of a cross-section plane is shown by a dashed line in Fig. 2, *b*). The layers from bottom to top: the silicon substrate; the Al_2O_3 buffer layer; the lower niobium electrode; the anode oxide for preventing short-circuits in the Josephson contacts and protecting the niobium surface when the junctions are formed; the thin aluminum layer of 6 nm; the AlO_x tunnel barrier; the upper niobium layer in the junctions; the silicon oxide insulation layer; the normal-metal (molybdenum) layer; the upper niobium electrode.

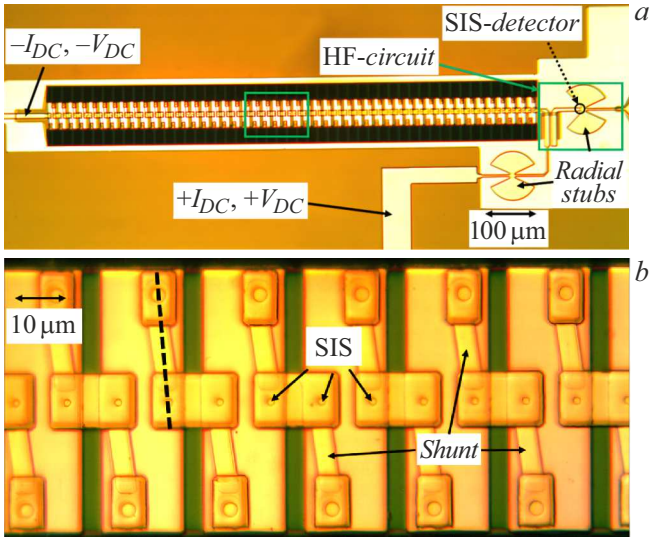

Figure 2. Optical microphoto of the array of the 100 shunted junctions (*a*) and the magnified image of the shunted SIS junctions in the array (*b*).

resistor made of a normal metal (molybdenum). In all the samples, the array is embedded into the central electrode of the coplanar line. Several series of the oscillator samples were manufactured [31] with a different current density in the arrays that consist of the 100, 200 and 350 junctions of the area of 2.8 and 4.2 μm^2. The junctions of the area of 2.8 and 4.2 μm^2 are shunted with resistors of resistance of 1.5 and 1 Ω, while the critical current of the junctions with the tunnel current density of 5 kA/cm^2 is 110 and 170 μA, respectively.

A high-frequency alternating signal generated by the array is detected and studied by means of an integrated detector on a single SIS junction arranged together with the array in the chip (the SIS-detector, Fig. 2, *a*). In order to independently measure the current-voltage curves of the array and the detector, their matching circuit is provided with a direct current block as a slot antenna (HF-circuit, Fig. 2, *a*). A radial stub (Fig. 2, *a*, to the right) is required for detuning of capacitance of the SIS detector. If the array is connected by direct current as a standard microstrip line, then a large portion of power of the HF signal flows into this line at its resonance frequencies and is not recorded by the detector. In order to reduce the influence of the direct current connection line on the HF signal, at a distance of a quarter of the wavelength from an edge of one of the electrodes of the slot antenna the line is provided with another radial stub (to the left of the HF-circuit, Fig. 2, *a*); it ensures high line impedance in the connection point at the operating frequency.

Implementation of stable oscillation at a certain frequency requires a unhysteretic nature of the current-voltage curve of each junction. Hysteresis occurs on the current-voltage curve due to the fact that the junction has finite capacitance; a hysteresis degree is characterized by the McCumber parameter β_c. In order to implement the unhysteretic nature of the current-voltage curve, the McCumber parameter β_c shall be below a certain value of about unity, wherein its exact value depends on a model that describes the Josephson junction [14]. The value of β_c may be calculated using the formula

$$\beta_c = 2eI_cR_J^2C/\hbar, \qquad (1)$$

where I_c — the critical current, $\hbar = h/2\pi$, R_J — the sub-gap resistance, C — the capacitance of the junction. For our case, the most adequate is a microscopic tunnel junction model (TJM) [14]. This model specifies that in order to obtain the unhysteretic current-voltage curve, the value of the McCumber parameter, which is determined according to the formula (1), shall be below 0.3. Due to using the shunt, for the SIS junctions in the array there is the value $\beta_c \sim 0.28$ for the junctions of the area of 2.8 μm^2 and $\beta_c \sim 0.2$ for 4.2 μm^2, which allowed obtaining an almost unhysteretic current-voltage curve.

It is shown in the paper [31] that within the framework of the RLCSJ-model it is possible to obtain a calculated current-voltage curve that is very close to an experiment. It was found during HFSS simulation of the junction characteristics that specific features on the experimental current-voltage curve are related to excitation of resonance due to capacitance of the junction and inductance of the shunt. The presence of the SIS junction is simulated by means of a boundary condition as described in the paper [32]. The used parameters of the RLCSJ model of the single junction Nb–AlN–NbN of the area of 2.8 μm^2 with the tunnel current density of ~ 13 kA/cm^2: the shunt resistance $R_s \approx 0.9$ Ω, the shunt capacitance $L \approx 1.7$ pH, the total capacitance of the structure is 0.361 pF.

3. Measurements and optimization of the design of the oscillator arrays

The first stage included investigation of various options of the design of the oscillator arrays [31], which include 100, 200 and 350 Josephson junctions with the tunnel current densities of 5, 13 and 20 kA/cm^2 (the photo of the array of the 100 Josephson junctions is shown in Fig. 2). In the batches with the junctions' tunnel current density of 5 kA/cm^2, the width of the operating band is caused by a characteristic of transmission of the matching circuit. In the samples with the high tunnel current density, the oscillation band turned out to be significantly narrower.

We have studied frequency dependences of the detector pump current for the samples with the arrays of the 350 junctions of the area of 2.8 and 4.2 μm^2. The maximum operating frequency of the array with the large-area junctions turned out to be somewhat lower, most likely, due to large spurious capacitance of the junctions. On average, oscillation power is higher in the array with the larger-area junctions, but the peak power turned out to be almost the same for the compared samples. It is found for the samples with $N = 100$, 200 and 350 junctions Nb–AlO_x–Nb (the tunnel current density is ~ 5 kA/cm^2 and the area is 2.8 μm^2) that with increase of the number of the junctions in the array the maximum oscillation power increases faster than N. Irregularity of the dependences is most likely related to origination of standing waves in the line and capture of the frequency in the respective operating points. In the sample with the 350 junctions, irregularity is most pronounced due to larger oscillated power and, respectively, larger efficiency of the frequency lock. Besides, there was a dip at the frequencies near 500 GHz, which is due to return of the power into the array's direct current connection line.

The region with maximum pump from 200 to 450 mV clearly exhibited resonance steps. A frequency distance between the steps is approximately $\Delta f \sim 20$ GHz both for the array with the junctions area $S = 2.8\,\mu$m^2 and $S = 4.2\,\mu$m^2. It is known that effective permittivity of the coplanar line is [33]:

$$\varepsilon^{\text{eff}} = (\varepsilon + 1)/2, \tag{2}$$

where $\varepsilon \sim 11.7$ is relative permittivity of the silicon substrate. The frequency interval between the resonances in the coplanar line can be evaluated by the formula

$$\Delta f \approx \frac{c}{\sqrt{\varepsilon^{\text{eff}}}2L}. \tag{3}$$

The length L of the line of the 350 junctions in the sample is 3500 μm, c — the speed of line in vacuum. Taking into account (2), the calculation according to the formula (3) gives $\Delta f \sim 17$ GHz, thereby making it possible to state that the steps observed on the current-voltage curve are most likely related to the geometrical resonances along the entire length of the coplanar line, in which the array

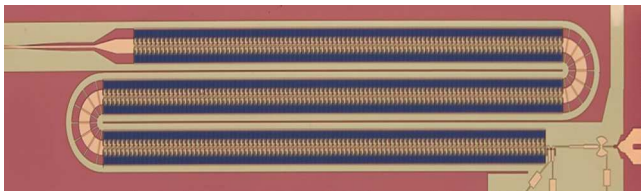

Figure 3. Photo of the optimized array of the 600 shunted junctions.

embedded. A small difference can be caused by additional capacitance and inductance, which occur in the line due to the SIS junctions and the shunts, and frequency dispersion of effective permittivity in the coplanar line.

In order to eliminate the above-listed problems (the standing waves and return of the power into the array's direct current connection line), we have designed samples with a match load at a non-emitting array end and an optimized design of supply of feed currents. The topology of the new structures was optimized in the Ansys HFSS three-dimensional numerical simulation software. A method of simulation of the superconducting structures in the Ansys HFSS software is described in detail in the papers [32,34]. Fig. 3 shows the photo of the optimized oscillator array that contains the 600 Josephson junctions. In addition to the concerted load at a left edge of the array, spurious reflections are reduced by providing the design with additional connections of external electrodes of the coplanar lines at the turns (similar to the air bridge).

When the SIS detector is affected by an external variable signal, probability of tunneling of quasi-particles is increased due to photons absorption, whence the current-voltage curve exhibits typical current steps. In this case the current-voltage curve can be described by means of expressions from the Tucker-Feldman model [1]:

$$I(V_0, V_f) = \sum_{n=-\infty}^{\infty} J_n^2\left(\frac{eV_f}{hf}\right) I_{DC}\left(V_0 + \frac{nhf}{e}\right), \tag{4}$$

where V_0 — voltage in the operating point, V_f — the amplitude of voltage of the external variable signal, f — the signal frequency, h — the Planck constant, e — the charge of the electron, n — the step number (the number of photons that participate in a process of interaction with one electron), $J_n(\alpha)$ — the Bessel functions of the first kind, $I_{DC}(V)$ — the current-voltage curve of the SIS junction without external radiation. By approximating a form of the current-voltage curve with the expression (4), it is possible to determine the frequency and V_f as well as the signal power with accuracy better than 3 %. Fig. 4 shows the current-voltage curves of the detector at the various frequencies of the external signal. A current value at the quasi-particle step in the operating point V_0, which is usually selected at the voltage a little less than the gap voltage is called the pump current I_{pump}. At the frequency of 411 GHz (the blue curve), the value of recorded power

was 0.4 μW, which is already enough for application in the superconducting integrated receivers [11,29].

If the critical current through the SIS detector is suppressed incompletely, then in addition to the quasi-particle steps the current-voltage curve also exhibits the Shapiro steps (Fig. 4). The respective voltages are determined by the formula

$$V_{Shapiro} = hfn/2e, \quad (5)$$

where f — the frequency of the external signal, n — the step number. The first and second Shapiro steps are observed in Fig. 4 at the frequencies of 320, 411 and 516 GHz; while the steps are still visible above the gap V_g, for example at the frequency of 411 GHz there is clearly the fifth step (the voltage of 4.25 mV) and even the sixth step (5.1 mV). By a position of the Shapiro steps, it is possible to determine the signal frequency with higher accuracy than by the position of the quasi-particle steps.

The current-voltage curve of the array of the 600 junctions is shown in Fig. 5 at the voltages below 800 mV; a color marks the pump current of the SIS detector. The current-voltage curve exhibits weakly pronounced current steps (see the insert). Fig. 6 shows a dependence of the pump current of the SIS detector on the frequency of the oscillator on the array of the 600 Josephson junctions with a matching circuit between the array and the SIS detector, which is optimized within the range 300–550 GHz. The red dashed curve marks a coefficient S_{21} of the matching circuit between the array and the SIS detector, which is calculated in Ansys HFSS. It is clear that the design is optimized so as to significantly extend the operating range of the oscillator. Moreover, a depth of resonances due to reflections from the array edges does not exceed 1.5 dB in the major part of the range; while reflections from the array turns are small and

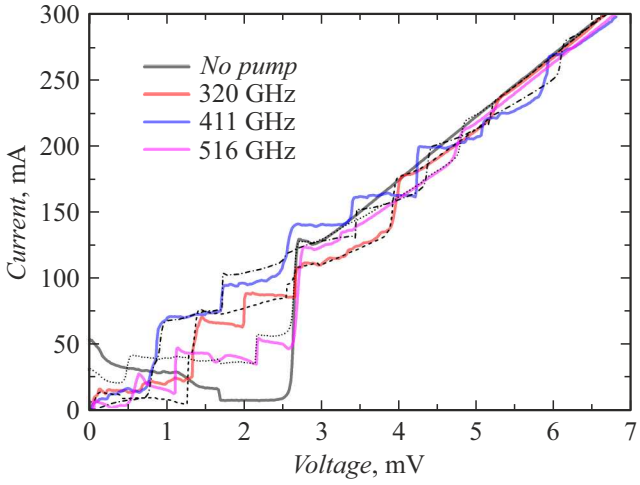

Figure 4. Family of the current-voltage curves of the SIS detector at the various frequencies of the signal from the array; the critical current is partially suppressed by the external magnetic field (320 GHz — the red curve, 411 GHz — the blue curve, 516 GHz — the purple curve). The dashed curves mark results of calculations according to the formula (4) when using the experimentally-measured autonomous current-voltage curve.

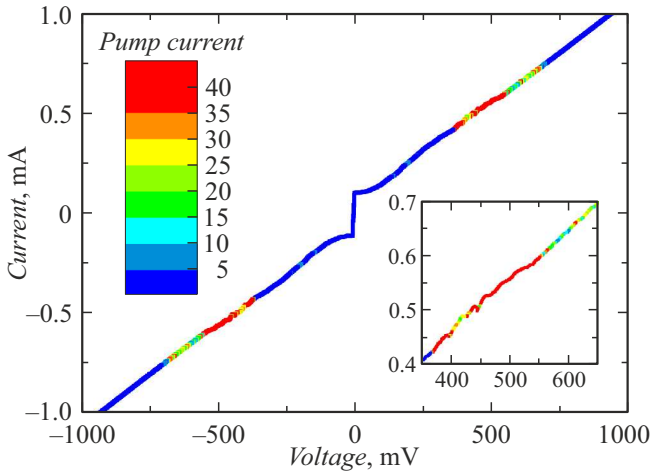

Figure 5. Current-voltage curve of the array of the 600 shunted Josephson junctions of the area of 2.8 μm^2. The value of the pump current in each point of the current-voltage curve is shown by the color. The insert shows a portion of the current-voltage curve within voltages that correspond to the frequency region 300–550 GHz.

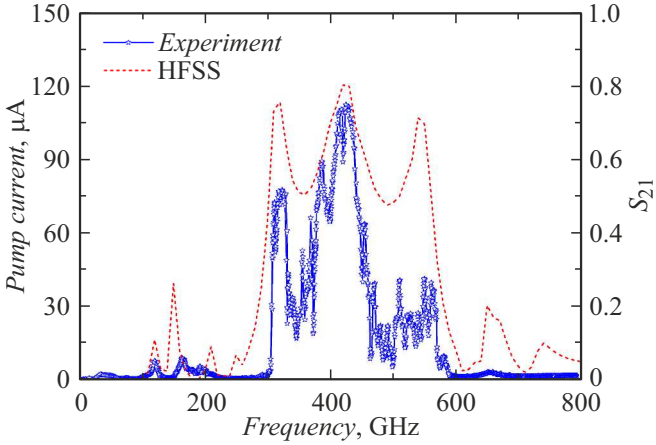

Figure 6. Dependence of the pump current on the oscillation frequency of the array that includes the 600 Josephson junctions of the area of 2.8 μm^2. The red dashed curve marks the coefficient S_{21} of the matching circuit between the array and the SIS detector, which is calculated in Ansys HFSS.

do not manifest themselves at the dependence of the pump current of the SIS mixer on the frequency.

The position of the Shapiro steps was taken to find that the oscillation frequencies that are calculated by the Josephson formula in terms of one junction and experimentally measured differ by several percent, which can be explained by incomplete synchronization of the junctions in the array due to complex dynamics of the processes in the system with a large number of the junctions [35].

The proposed topology of the arrays of the lumped Josephson junctions allowed creating the controllable retunable terahertz-range oscillator with power that is enough

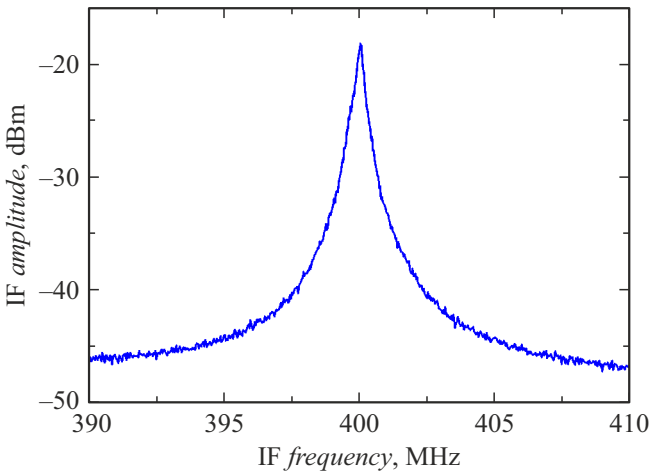

Figure 7. Radiation spectrum of the array of the 600 junctions at the frequency of 450 GHz, which is down-converted in frequency and measured with resolution of the spectrum analyzer (RBW) 180 kHz. The linewidth is 360 kHz; the signal-to-noise ratio is 29 dB.

for on-chip applications as the local oscillator in the superconducting integrated receiver. A radiation spectrum of the array of the shunted Josephson junctions was measured by using an integrated structure shown in Fig. 2. In the SIS detector, array radiation is mixed with harmonics of the signal from a synthesizer adjusted to the frequency 15–18 GHz; in this measurement the SIS detector operates as a harmonic mixer. The signal at the intermediate frequency is output from a cryostat to an input of the spectrum analyzer. Fig. 7 shows the radiation spectrum of the array of the 600 junctions; an autonomous linewidth is 360 kHz. The study [31] has demonstrated a capability of frequency and phase stabilization of the radiation frequency of these arrays at the frequencies of up to 650 GHz.

Conclusion

Summing up, we fabricated and studied the oscillators based on the arrays of the Josephson junctions connected in series and embedded into the central electrode of the coplanar line; each junction was shunted by the thin-film resistor made of normal metal. In the topology suggested, it was possible to achieve the radiation with continuous frequency tuning within the range 100–750 GHz. We also investigated the impact of the areas of the junctions on the output power of the array. For the array with the junctions area $S = 2.8\,\mu\text{m}^2$ pump of the SIS-detector at frequencies up to 700 GHz was observed. With increase in the number of junctions in the array, the power recorded by the detector increases.

We also optimized the array design that allowed to significantly expand the operating frequency range of the oscillator to improve the uniformity of the output power; the depth of the resonances due to the reflections from array edges does not exceed 1.5 dB in a major part of the range. The peak power of the detector was $0.4\,\mu$W; it is sufficient for the on-chip application in the superconducting integrated circuits. The present study is a step on the way to the superconducting local oscillator based on the arrays of the shunted Josephson junctions connected in series, where the array is embedded into the central electrode of the coplanar line. Furthermore, there are a few methods for further increasing its radiation power.

Compared to the long Josephson junctions, the arrays in proposed topology have an important advantage in operation at subTHz frequencies that is smaller impact of the surface losses in the superconducting electrodes due to another configuration of high-frequency currents which flow directly in the area of LJJ. The coplanar line enables the fabrication of the electrodes from the materials with higher critical temperatures and the gap voltage (therefore, with smaller surface losses at frequencies about 1 THz). The Josephson tunnel junctions meanwhile can be formed based on well-established technologies. At the same time, it is possible to use the tunnel junctions with the very high current density despite significant deterioration of the quality parameter since the junctions in the proposed design are shunted by the thin-film resistor in order to suppress the hysteresis of the current-voltage curve. Moreover, use of the self-shunted junctions (e.g., [36]) would allow to reduce parasitic shunt inductance and further extend the operating range to high frequencies.

Funding

This study was supported by the Ministry of Science and Higher Education of the Russian Federation (Agreement № 075-15-2024-538).

Conflict of interest

The authors declare that they have no conflict of interest.

References

[1] J.R. Tucker, M.J. Feldman. Rev. Modern Phys., **57** (4), 1055 (1985). DOI: 10.1103/RevModPhys.57.1055
[2] A.R. Kerr, M.J. Feldman, S.-K. Pan. *Proceedings of the Eighth International Symposium on Space Terahertz Technology* (Cambridge, MA, USA, 1997)
[3] *Apex Space Telescope Website*. Available online: http://www.apex-telescope.org
[4] *LLAMA Space Observatory Website*. https://www.llamaobservatory.org/
[5] *Hershel Space Telescope Website*. Available online: https://www.herschel.caltech.edu/
[6] *„Millimetron“ space observatory website*. Available online: https://millimetron.ru/

[7] G. de Lange, M. Birk, D. Boersma, J. Dercksen, P. Dmitriev, A.B. Ermakov, L.V. Filippenko, H. Golstein, R.W.M. Hoogeveen. L. de Jong. Supercond. Sci. Tech., **23** (4), 045016 (2010). DOI: 10.1088/0953-2048/23/4/045016
[8] V.P. Koshelets, S.V. Shitov, A.B. Ermakov, L.V. Filippenko, O.V. Koryukin, A.V. Khudchenko, M.Yu. Torgashin, P.A. Yagoubov, R.W.M. Hoogeveen, O.M. Pylypenko. IEEE Trans. Appl. Supercond., **15** (2), 960 (2005). DOI: 10.1109/TASC.2005.850138
[9] J.V. Siles, K.B. Cooper, C. Lee, R.H. Lin, G. Chattopadhyay, I. Mehdi. IEEE Transactions Terahertz Sci. Technol., **8** (6), 596 (2018). DOI: 10.1109/TTHZ.2018.2876620
[10] J.V. Siles, A.E. Maestrini, C. Lee, R. Lin, I. Mehdi. IEEE Transactions Terahertz Sci. Technol., **14** (5), 607 (2024). DOI: 10.1109/TTHZ.2024.3430013
[11] L.V. Filippenko, A.M. Chekushkin, M.Yu. Fominskii, A.B. Ermakov, N.V. Kinev, K.I. Rudakov, A.V. Khudchenko, A.M. Baryshev, V.P. Koshelets, S.A. Nikitov. Phys. Usp., **67**, 1139, (2024). DOI: 10.3367/UFNe.2024.07.039726
[12] V.P. Koshelets, P.N. Dmitriev, M.I. Faley, L.V. Filippenko, K.V. Kalashnikov, N.V. Kinev, O.S. Kiselev, A.A. Artanov, K.I. Rudakov, A. de Lange, G. de Lange, V.L. Vaks, M.Y. Li, H. Wang. IEEE Trans. Terahertz Sci. Technol., **5** (4), 687 (2015). DOI: 10.1109/TTHZ.2015.2443500
[13] D.R. Gulevich, V.P. Koshelets, F.V. Kusmartsev. Phys. Rev. B, **96** (2), 024515 (2017). DOI: 10.1103/PhysRevB.96.024515.
[14] K.K. Likharev. *Dynamics of Josephson junctions and circuits*. (Gordon and Breach science publishers, NY., 1986)
[15] D.D. Coon, M.D. Fiske. Phys. Rev., **138** (3A), A744 (1965). DOI: 10.1103/PhysRev.138.A744
[16] Y. Uzawa, S. Saito, W. Qiu, K. Makise, T. Kojima, Z. Wang. J. Low Temperature Phys., **199**, 143 (2020). DOI: 10.1007/s10909-019-02324-1
[17] A.K. Jain, K.K. Likharev, J.E. Lukens, J.E. Sauvageau. Phys. Reports, **109** (6), 309 (1984). DOI: 10.1016/0370-1573(84)90002-4
[18] P. Barbara, A.B. Cawthorne, S.V. Shitov, C.J. Lobb. Phys. Rev. Lett., **82** (9), 1963 (1999). DOI: 10.1103/physrevlett.82.1963
[19] M. Darula, T. Doderer, S. Beuven. Supercond. Sci. Tech., **12** (1), R1 (1999). DOI: 10.1088/0953-2048/12/1/001
[20] M.A. Galin, V.V. Kurin, I.A. Shereshevsky, N.K. Vdovicheva, A.V. Antonov, B.A. Andreev, A.M. Klushin. IEEE Trans. Appl. Supercond., **31** (5), 1 (2021). DOI: 10.1109/TASC.2021.3064533
[21] P.A.A. Booi, S.P. Benz. Appl. Phys. Lett., **68** (26), 3799 (1996). DOI: 10.1063/1.116621
[22] A. Kawakami, Y. Uzawa, Z. Wang. IEEE Trans. Appl. Supercond., **9** (2), 4554 (1999). DOI: 10.1109/77.784039
[23] B. Bi, S. Han, J.E. Lukens, K. Wan. IEEE Trans. Appl. Supercond., **3** (1), 2303 (1993). DOI: 10.1109/77.233544
[24] P.A.A. Booi, S.P. Benz. Appl. Phys. Lett., **64** (16), 2163 (1994). DOI: 10.1063/1.111984
[25] M.A. Galin, N.V. Kinev, M.Yu. Levichev, A.I. El'kina, A.V. Antonov, A.V. Khudchenko, G.P. Nazarov, V.V. Kurin, V.P. Koshelets. IEEE Trans. Appl. Supercond., **34** (3), (2024). DOI: 10.1109/TASC.2023.3337197
[26] J. Lukens. *Study of Josephson Effect Arrays as Sources at 1 THz* (Rome Air Development Center, Air Force Systems Command, Rome, 1990). p. 110.
[27] L.V. Filippenko, S.V. Shitov, P.N. Dmitriev, A.B. Ermakov, V.P. Koshelets, J.R. Gao. IEEE Trans. Appl. Supercond., **11** (1), 816 (2001). DOI: 10.1109/77.919469
[28] P.N. Dmitriev, I.L. Lapitskaya, L.V. Filippenko, A.B. Ermakov, S.V. Shitov, G.V. Prokopenko, S.A. Kovtonyuk, V.P. Koshelets. IEEE Trans. Appl. Supercond., **13** (2), 107 (2003). DOI: 10.1109/TASC.2003.813657
[29] K.I. Rudakov, A.V. Khudchenko, L.V. Filippenko, M.E. Paramonov, R. Hesper, D.A.R. da Costa Lima, A.M. Baryshev, V.P. Koshelets. Appl. Sci., **11** (21), 10087 (2021). https://doi.org/10.3390/app112110087
[30] *Unique Research Faciity „Kriointegral“–„Technology and Measurement Facility for Fabrication of Superconducting Nanosystems using New Materials“* Electronic source. Available at: http://www.cplire.ru/rus/kriointegral/index.html; http://ckp-rf.ru/usu/352529/
[31] F.V. Khan, L.V. Filippenko, A.B. Ermakov, M.E. Paramonov, M.Yu. Fominskii, N.V. Kinev, V.P. Koshelets, S.A. Nikitov. UFN, **195** (6), 621 (2025) (in Russian). DOI: 10.3367/UFNr.2024.12.039864
[32] F.V. Khan, L.V. Filippenko, V.P. Koshelets. J. Commun. Technol. Electron., **68** (9), 983 (2023). DOI: 10.1134/S1064226923090115
[33] R. Garg, I. Bahl, M. Bozzi. *Microstrip lines and slotlines* (Artech house, 2013)
[34] V. Belitsky, C. Risacher, M. Pantaleev, V. Vassilev. Intern. J. Infrared Millimeter Waves, **27**, 809 (2006). DOI: 10.1007/s10762-006-9116-5
[35] M.A. Galin, I.A. Shereshevsky, N.K. Vdovicheva, V.V. Kurin. Supercond. Sci. Technol., **34** (7), 075005 (2021). DOI: 10.1088/1361-6668/abfd0b
[36] S.K. Tolpygo, R. Rastogi, T. Weir, E.B. Golden, V. Bolkhovsky. IEEE Trans. Appl. Supercond., **34** (3), (2024). DOI: 10.1109/TASC.2024.3364128

Translated by M.Shevelev

Translated by M.Shevelev